

COMPARISON OF TURBULENT MODELS FOR CANDU MODERATOR FOLLOWING A PRESSURE TUBE TO CALANDRIA TUBE CONTACT

A. BEHDADI, J.C. LUXAT

McMaster University, Engineering Physics Department, Hamilton, Ontario, Canada L8S 4L7
e-mail: behdada@mcmaster.ca; luxatj@mcmaster.ca

ABSTRACT

In this paper, the CANDU moderator flow and temperature distribution have been studied by developing a Computational Fluid Dynamics (CFD) model. The model predicts the fluid velocity and temperature distribution around a channel in normal operation and also after a postulated ballooning deformation of the pressure tube (PT) into contact with its calandria tube (CT). The present research is focused on establishing the limits for dryout occurrence on the CTs after PT/CT contact. CT dryout may occur due to the large spike of heat flux to the moderator after contact. The CT post-dryout temperature may become sufficiently high to result the thermal creep strain deformation and affect the channel integrity. In this study two different turbulent models, standard $k - \varepsilon$ and $k - \omega$, have been used and compared in order to consider turbulence in moderator flow. Governing equations have been solved by the finite element software package COMSOL. The buoyancy driven natural convection, the local moderator subcooling, fluid velocity, wall temperature and heat flux has been analyzed in the model. The flow pattern and temperature distribution predicted by both turbulent models indicate a greater tendency for film boiling to occur at low subcoolings and at the top or bottom of the CT.

1. INTRODUCTION

The CANDU reactor safety research program in Canada has a strong focus on developing and verifying computer models that predict the reactor process and safety systems accurately during accident situations. Heavy water moderator surrounding each fuel channel is one of the important features in CANDU reactors that acts as a heat sink for the fuel in the situations where other means of heat removal fail. A loss of Coolant Accident (LOCA) caused by a break in one of the primary heat transport system pipes is one of the most safety significant accidents in water reactors and can be the precursor to more serious accidents. During postulated LOCAs, for a particular break size and location referred to as critical break LOCA, the coolant flow through a portion of the reactor core stagnates before the emergency coolant injection restores fuel cooling. In addition, the emergency coolant injection system may fail to operate. In such cases, fuel cooling becomes severely degraded due to rapid flow reduction in the affected flow pass of the heat transport system. This can result in pressure tubes experiencing significant heatup while coolant pressure is still high, thereby causing uniform thermal creep strain (ballooning) of the PT into contact with its CT^[14]. Contact of the hot PT with the CT leads to rapid redistribution

of stored heat from the PT to CT and a large spike in heat flux from the CT to the moderator fluid. For lower subcooling conditions of the moderator, dryout of the CT can occur. The focus of this research is to establish a Computational Fluid Dynamics (CFD) model for predicting the moderator flow field and temperature distribution around one single channel to investigate the potential of dryout occurrence on the CT surface following a PT/CT contact.

Experimental studies on the flow and temperature distribution inside the moderator have been performed in Canada since the early 1980s. The moderator temperature was measured by Austman et.al.^[2]. They inserted thermo-couples through a shut-off rod guide tube in operating CANDU reactors at Bruce A and Pickering. In the Stern Laboratories in Canada, Huget et.al.^[7,8] performed 2D moderator circulation tests. They observed three distinct flow patterns. Khartabil et.al.^[11] performed 3D moderator circulation tests in the moderator temperature facility (MTF) in the Chalk River Laboratories of Atomic Energy of Canada Limited. These tests had been conducted along with separate effect tests such as a hydraulic resistance through tube bundles, velocity profiles at an inlet diffuser, flow development along a curved wall and the turbulence generation by temperature differences. Gillespie^[6] described a simple one dimensional model for thermal behavior of a fuel channel when the internal pressure is high enough to deform the PT into contact with its CT. He compared these predictions with his related experimental results and developed the computer program WALLR. In this program the transient heat conduction equation between the pressure tube and calandria tube is solved in the radial direction by a standard one dimensional, finite element subroutine called WALL. For the boundary conditions he specified a heat flux on the inside surface of the pressure tube. Comparing the model predictions with the experimental results, the author concluded that the computer program WALLR predictions for the experiments with an internal pressure of more than 1MPa is qualitatively accurate. Szymanski et.al.^[16] developed a thermal-hydraulic code, called MODTURC as a modification of the older code MODCIR^[1,3], to calculate the moderator temperature and velocity distribution in the calandria of a CANDU reactor. They used the finite difference technique and $k - \varepsilon$ turbulence model to solve three dimensional equations for one quarter of the vessel which was assumed to be symmetric. They also compared the code predictions to experimental results of one reactor design and found a better agreement than previous predictions without turbulence modeling.

Based on these works, a CFD code MODTURC-CLAS (Moderator TURbulent Circulation Co-Located Advanced Solution) has been developed by Ontario Power Generation (OPG) and selected as a component of the Canadian Industry Standard Toolset (IST) for safety analysis. On the other hand, CFD models based on commercial software packages have been developed by others for predicting the CANDU-6 moderator temperature. Kim et.al.^[12] investigated the moderator thermalhydraulic characteristics using the FLUENT code. They modeled all the calandria tubes as heating pipes without any approximation for the core region and investigated the moderator thermalhydraulic characteristics using their optimized model. The authors predicted three flow patterns inside the moderator, i.e., momentum dominated flow, buoyancy dominated flow and mixed type flow depending on the inlet flow rate, heat load, or both. They concluded that since the moderator has enough coolability as the alternate heat sink, the flow pattern does not undergo significant changes, the fuel channel integrity can be assured, and no boiling occurs.

The computer programs developed to assess the effect of heat transfer on the CT surface after a postulated PT/CT ballooning contact such as WALLR^[6] and CATHENA^[5] are one-dimensional codes and predict film boiling completely around the circumference of the CT. This does not happen in the experiments. In the experiments the calandria tube surface had patches of film boiling surrounded by patches of nucleate boiling. Therefore in this study the simulation has been performed in two dimension. In addition, in other studies in 2D or 3D, the whole calandria has been modeled. However, it is a concern that when PT/CT contact occurs in a channel, local moderator boiling may lead to CT dryout and may affect the flow around the CTs at higher elevations. This can detrimentally affect channel integrity if the CT post-dryout temperature becomes sufficiently high to result in thermal creep strain deformation. According to the importance of local prediction of flow and temperature distribution around a single channel, this study has been performed in order to investigate the local thermalhydraulic conditions on the calandria tube wall that will influence potential dryout. This problem has been analyzed using the general purpose finite element code COMSOL.

2. MODEL DESCRIPTION

In this model, a single phase fluid inside the moderator and a uniform PT/CT contact has been considered. During normal operation, heat can be deposited to the moderator in two different ways. The first one is by direct heating of neutrons, decay heat from fission products and gamma rays. The second way, which accounts for a small portion of the total heat load, is by heat convection from the surface of fuel channels. The total heat load to the moderator is taken to be 103 MW (about 103% of full power) consisting of 98.7 MW by volumetric direct heating and 4.3 MW by convective heat from fuel channel surface^[12]. The convective heat transfer to the moderator is assumed to be uniformly with axial direction.

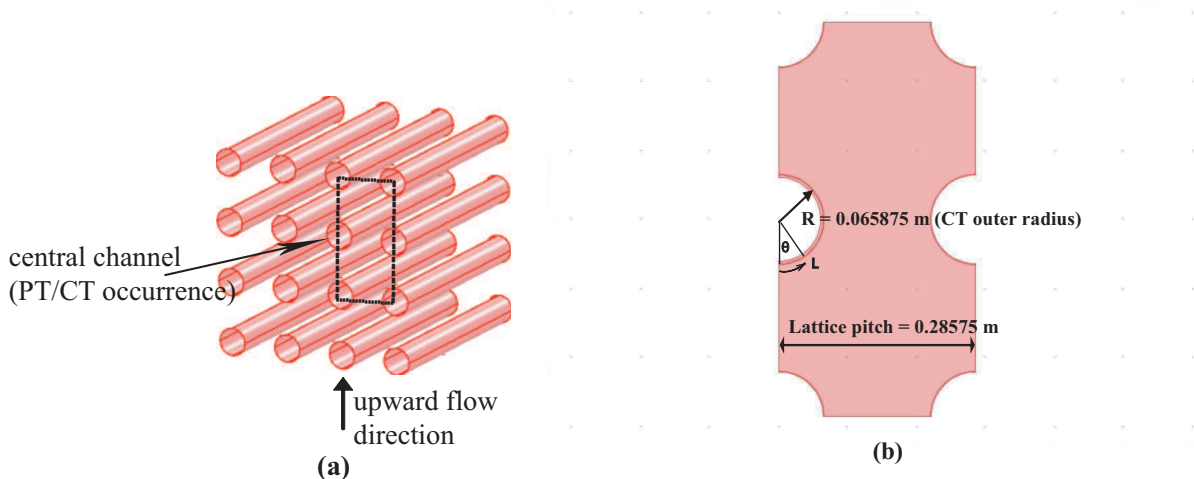


Figure 1. a) part of calandria tubes in 3D, b) the model geometry in 2D

The geometry is depicted in Figure 1-a. The arrow indicates the flow direction for upward

flow. Neglecting any end effects from the walls of the vessel, the solution is constant in the direction of the tubes and therefore the model is reduced to a 2D domain. The dashed line marks the model region in 2D which is shown in Figure 1-b. L denotes the arc-length associated with the angle θ on the surface of the central CT in which PT/CT contact is postulated to occur. The effect of neighboring channels on the flow field is taken into account by including part of them into the domain.

3. GOVERNING EQUATIONS

The standard $k - \epsilon$ or $k - \omega$ turbulence model associated with a logarithmic wall function is used to predict the turbulence. The governing equations in this model are:

- Reynolds Averaged Navier-Stokes (RANS) equations in the heavy water moderator domain:

$$\frac{D\rho}{Dt} + \rho \nabla \cdot \mathbf{u} = 0 \quad (1)$$

$$\rho \frac{D\mathbf{u}}{Dt} = \mathbf{F} - \nabla p + (\mu + \mu_T) [\nabla^2 \mathbf{u} + \frac{1}{3} \nabla (\nabla \cdot \mathbf{u})] \quad (2)$$

- Transport equations of the turbulence models^[18]

$k - \epsilon$ **transport equations:**

$$\rho \frac{Dk}{Dt} = -\nabla \cdot [\mu + \frac{\mu_T}{\sigma_k} \nabla k] = \frac{1}{2} \mu_T \nabla^2 \mathbf{u} - \rho \epsilon \quad (3)$$

$$\rho \frac{D\epsilon}{Dt} - \nabla \cdot [\mu + \frac{\mu_T}{\sigma_\epsilon} \nabla \epsilon] = \frac{1}{2} C_{\epsilon 1} \frac{\epsilon}{k} \mu_T \nabla^2 \mathbf{u} - \rho C_{\epsilon 2} \frac{\epsilon^2}{k} \quad (4)$$

$k - \omega$ **transport equations:**

$$\rho \frac{Dk}{Dt} = -\nabla \cdot [\mu + \mu_T \sigma_k \nabla k] + \frac{1}{2} \mu_T \nabla^2 \mathbf{u} - \rho \beta_k k \omega \quad (5)$$

$$\rho \frac{D\omega}{Dt} = -\nabla \cdot [\mu + \mu_T \sigma_\omega \nabla \omega] + \frac{\alpha}{2} \mu_T \frac{\omega}{k} \nabla^2 \mathbf{u} - \rho \beta \omega^2 \quad (6)$$

- Heat transport equation in the water domain and the solid tube walls (CT thickness):

$$\rho C_p \frac{DT}{Dt} = \nabla \cdot ((k + k_T) \nabla T) + Q \quad (7)$$

Where,

\mathbf{u} is the velocity field, [m/s]

\mathbf{F} is body force, [N/m³]

p is pressure, [Pa]
 ρ is fluid density, [kg/m^3]
 μ is dynamic viscosity, [Pa.s]
 ∇ is vector differential operator
 μ_T is turbulent viscosity, [Pa.s]
 k is the turbulent kinetic energy, [m^2/s^2]
 ϵ is the dissipation rate of turbulence energy, [m^2/s^3]
 k is the fluid thermal conductivity, [$W/(m.K)$]
 t is time, [s]
 κ_T is turbulence thermal conductivity ($\frac{C_p \mu_T}{Pr_T}$), [$W/(m.K)$]
 C_p is specific heat capacity, [$J/(kg.K)$]
 Pr_T is turbulent Prandtl number
 Q is the heat source, [W/m^3]
 I is the identity matrix.

The model constants in the above equations are determined from experimental data^[18]; their values for $k - \epsilon$ model are: $C_\mu = 0.09$, $C_{\epsilon 1} = 1.44$, $C_{\epsilon 2} = 1.92$, $\sigma_k = 1.0$, $\sigma_\epsilon = 1.3$. The heat source is the volumetric heat flux by direct heating of neutrons, decay heat from fission products and gamma rays. Free convection which is due to the density gradient, is added to the momentum balance in the body force term.

Logarithmic wall function has been used for solid walls in turbulent flow. In this approach, a constitutive relation between the velocity and surface shear stress replaces the thin boundary layer near the wall. These relations known as wall functions are accurate for high Reynolds numbers and situations where pressure variations are not very large along the wall. The idea of the wall functions approach^[13] is to apply boundary conditions some distance δ_w away from the actual wall, so that the turbulence model equations are not solved close to the wall. The flow is considered to be parallel to the wall. We define δ_w^+ which is the distance from the wall normalized by the viscous lengthscale l^* and is given by

$$\delta_w^+ = \frac{\delta_w}{l^*} = \frac{u_\tau \delta_w}{\nu} \quad (8)$$

where $\nu = \mu/\rho$ is the kinematic viscosity. The logarithmic wall functions are formally valid for values of δ_w^+ between 30 and 100. Referring to the logarithmic law of the wall^[17] the velocity can be described by

$$\mathbf{u}^+ = \frac{\mathbf{u}}{u_\tau} = \frac{1}{\kappa} \ln(\delta_w^+) + C^+ \quad (9)$$

where \mathbf{u}^+ is the mean velocity normalized by the friction velocity, κ denotes the Von Karman's constant (about 0.41) and C^+ is a universal constant (about 5.2 for smooth walls)^[15].

In order to model the temperature in the laminar boundary layer at the CT/liquid interface, a thermal wall function Equation (10) is applied which relates the resistance to heat transfer

through the laminar boundary layer to that for momentum transfer for the fluid. The heat flux is determined by^[4]:

$$q = \frac{\rho C_p C_\mu^{0.25} k_w^{0.5} (T_w - T)}{T^+} \quad (10)$$

where, ρ and C_p are the fluid density and specific heat capacity, respectively, C_μ is a numerical constant of the turbulence model, and k_w is the turbulent kinematic energy at the wall. Furthermore, T_w is the wall temperature while T is the fluid temperature. The quantity T^+ is related to the wall offset in viscous units, δ_w^+ , through the definition:

$$T^+ = \frac{Pr_T}{\kappa} \ln(\delta_w^+) + \beta \quad (11)$$

where the turbulent Prandtl number Pr_T is fixed to 0.85^[10], the Von Karman constant κ obtained from experiments is equal to 0.41^[15]. β is a model constant set to 3.27^[10]. The wall offset in viscous units is defined as:

$$\delta_w^+ = \frac{\delta_w C_\mu^{0.25} k_w^{0.5}}{\nu} \quad (12)$$

where, δ_w is specified wall offset which is considered as half the local mesh size at the boundary.

4. BOUNDARY CONDITIONS

Two groups of boundary conditions are applied to the model, one group is for the $k - \epsilon$ and $k - \omega$ Equations (1) to (6) in the fluid domain and the other group is for the heat transport Equation (7).

For Navier-Stokes equations in the fluid domain the specified boundary conditions are:

- A pressure difference between inlet and outlet given by the mass flow.
- Normal flow and stream-wise periodic conditions for velocity, at the inlet and outlet.
- Symmetry boundary condition at the region borders.

For the heat transport equation, the boundary conditions are specified as:

- Moderator temperature with different subcoolings at the inlet.
- Convection dominated transport at the outlet of the domain.

- At the inner surface of calandria tubes a heat flux associated with normal operation is implemented. While, in central one after a postulated PT/CT contact, the applied heat flux is increased with time until the saturation point is reached in the fluid.
- The borders of the domain are considered to be symmetric.

The above equations are solved simultaneously inside the domain shown in Figure 1-b using finite element method^[19] in order to find the unknowns ($\mathbf{u}(u, v), p, T, k, \epsilon$). The number of elements is 6230 with an unstructured mesh in accordance with the mesh sensitivity analysis. The number of degree of freedom is 58062.

5. RESULTS AND DISCUSSION

5.1 STEADY-STATE RESULTS

To obtain the initial values for the transient case, a steady-state problem has been solved first. In the steady-state case all six channels are in the normal operation and a heat flux associated with 4.3 MW of direct heating from fuel channel surface^[12] is applied. Figure 2 (a) shows the velocity streamlines in the domain. Red color is associated with high velocity regions, while, blue indicates the low velocity regions. From the velocity distribution one can conclude that fluid velocity is low at the top and at the bottom of the CTs. The flow field is periodic in the y direction. It is also shown that the velocity field in the domain is symmetric. Figure 2 (b) shows the velocity contours using periodic velocity conditions. It can be seen that the inflow and outflow velocity profiles match. It also shows the velocity profile at the inflow region.

5.2 TRANSIENT RESULTS

In the transient case, the applied heat flux to the central CT surface is increased with time until the saturation point is reached in the fluid. The Minimum time step used in the model is 0.001s. By further decreasing in time step, no significant change was observed. Heat is implemented uniformly to the inner surface of the tube and increases exponentially by time. After 1s it reaches to its maximum value at which the maximum fluid temperature around the cylinder is near saturation. The transient results are shown separately for $k - \epsilon$ and $k - \omega$ models.

5.2.1 $k - \epsilon$ model

Figure 3 shows the temperature distribution and velocity streamlines for an inlet flow velocity of 0.5m/s for both upward and downward flow. Arrows indicate the flow direction while the colors show the temperature distribution. Three different areas for the velocity field can be clearly seen: 1) the stagnation point in the front, 2) the recirculation zone in the rear behind the cylinder, 3) high velocity regions in the middle of the cylinder. The separation of the boundary layer from the cylinder surface occurs at $L \simeq 0.16$ or $\theta = 137$ degree, which is very close to the experimental as well as theoretical value of $\theta = 140$ degree^[9,20].

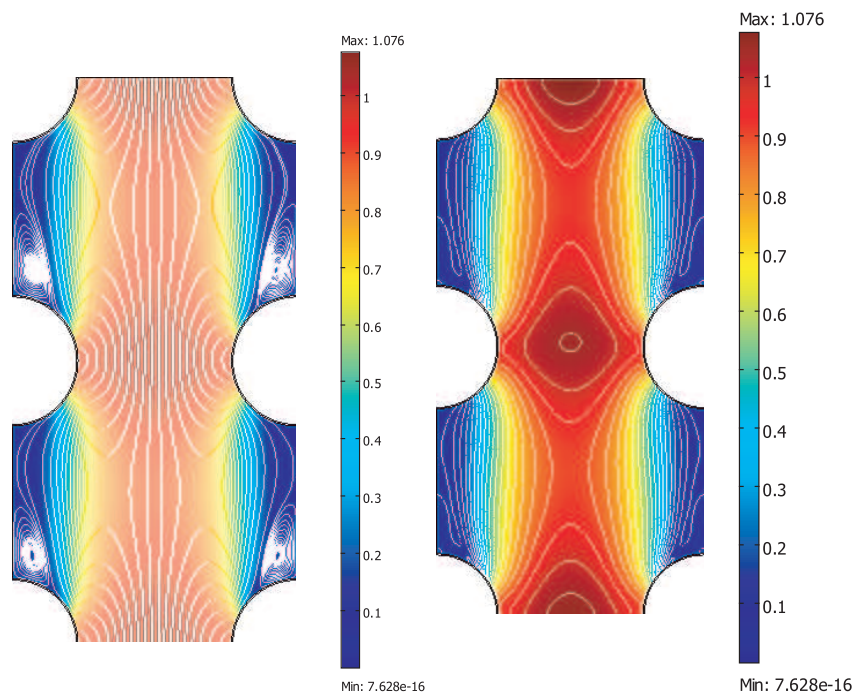


Figure 2. (a) velocity streamlines, (b) velocity contours, in the steady-state upward flow

Temperature distribution of the fluid around the central CT is shown in Figure 4 for different subcoolings of upward flow. Maximum temperature in the fluid is considered to be less than saturation. For each subcooling starting at the stagnation point $\theta = 0$ and $L = 0$, temperature decreases with increasing arc-length due to increase in velocity and heat transfer coefficient. However by developing the laminar boundary layer on the CT surface, the heat transfer coefficient decreases and temperature increases to its maximum value considered in this model. Eventually, separation occurs at $L = 0.16$ and fluid temperature declines due to the increase in heat transfer coefficient as a result of the considerable mixing associated with the wake region. However, as can be observed in the Figure 4 the variations in local fluid temperature become smaller as subcooling reduces. Qualitatively, this indicates a greater tendency for vapor film to extend around the CT surface as subcooling decreases. This signifies the importance of moderator fluid subcooling in the situation of critical break LOCA inside the CANDU reactor. As subcooling increases the region of high fluid temperature becomes increasingly localized which will result in higher likelihood of quenching. This makes the spreading of drypatches around the CT more difficult.

Figure 5 shows the temperature distribution around the central CT for downward flow with different subcoolings. Similar to the upward flow, the maximum fluid temperature is considered to be less than the saturation point. The same behavior as the upward flow can be seen in the downward situation. As it is shown in Figure 5 for each subcooling starting from the stagnation point which is at $\theta = 180$ and $L = 0.21$, due to the increase in fluid velocity and heat transfer coefficient, temperature decreases. By developing the laminar boundary layer, the heat transfer coefficient decreases and temperature increases to its maximum value. After the separation point around $L = 0.04$ due to the increase in heat transfer coefficient in the wake region, fluid

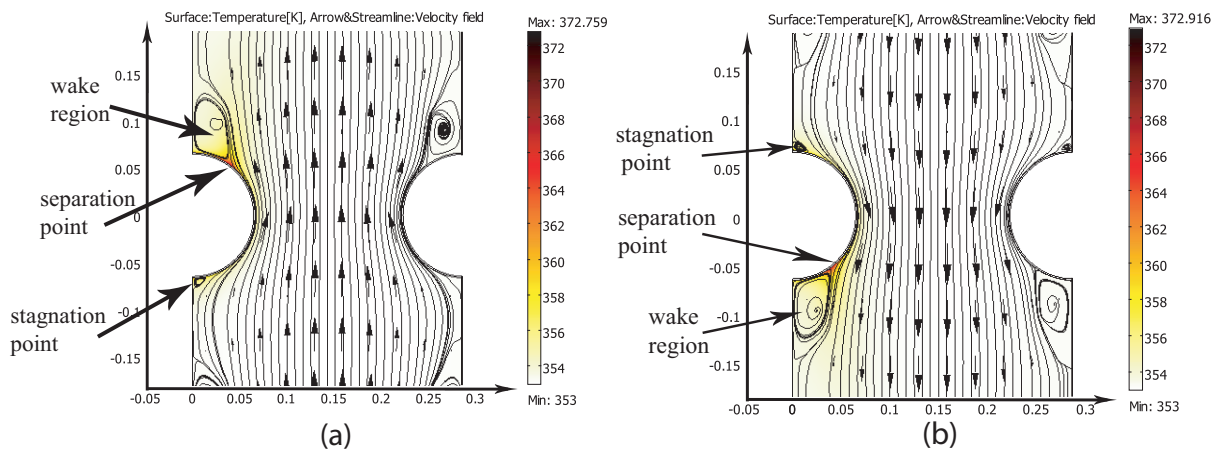


Figure 3. Velocity streamlines for (a) upward and (b) downward flows, $k - \epsilon$ model

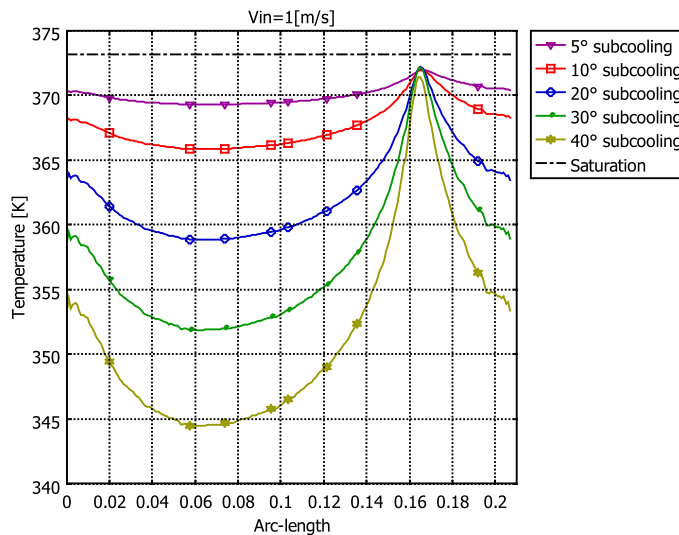


Figure 4. Local temperature around CT for upward flow by $k - \epsilon$ model

temperature decreases. Similar to the upward flow again it should be noted that as subcooling decreases, the variations in local fluid temperature become smaller and therefore it is more probable for the vapor film to extend around the CT surface at low subcoolings.

5.2.2 $k - \omega$ model

Figure 6 shows the temperature distribution and velocity streamlines in the domain for both upward and downward flow obtained by the $k - \omega$ model. It can be seen that in $k - \omega$ predictions, the wake region on the cylinder is larger than previous model.

Temperature distribution around the central CT for different subcoolings obtained by $k - \omega$ model is shown in Figures 7 and 8 for upward and downward flows respectively. Maximum

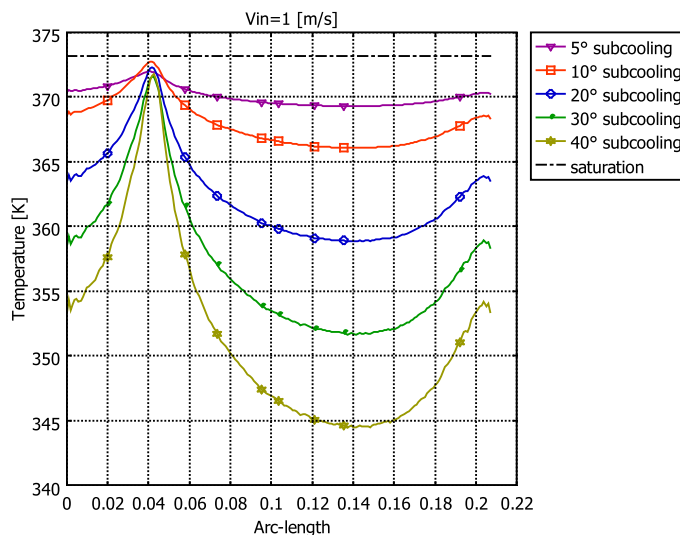


Figure 5. Local temperature around CT for downward flow by $k - \epsilon$ model

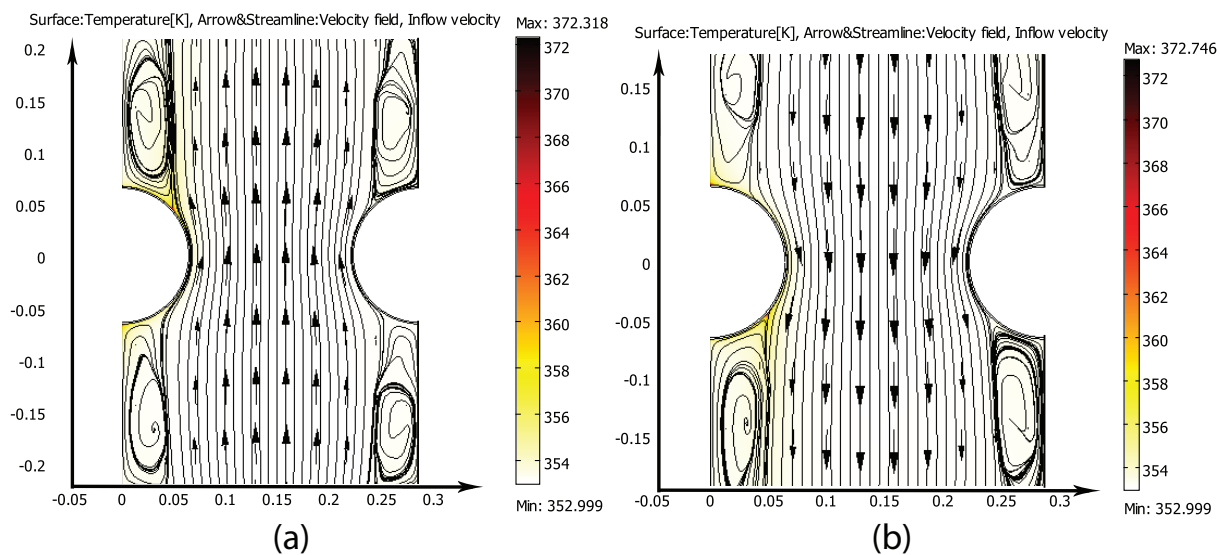


Figure 6. Velocity streamlines for upward and downward flows, $k - \omega$ model

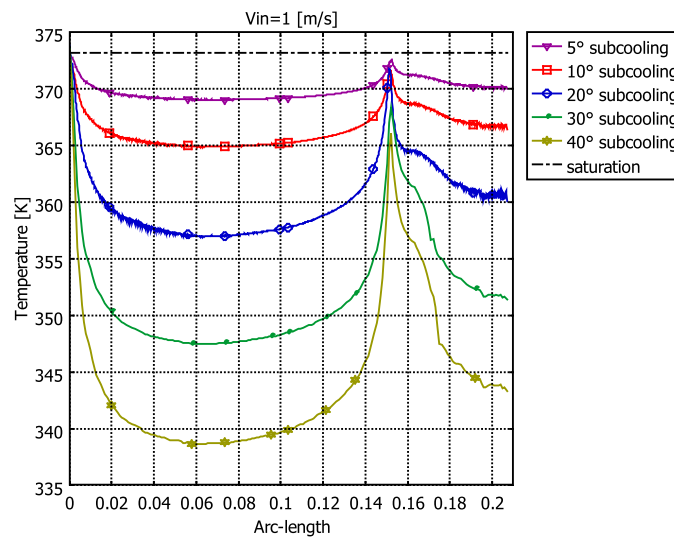


Figure 7. Local temperature around CT for upward flow by $k - \omega$ model

temperature in the fluid is considered to be less than saturation. The same as the $k - \epsilon$ model for each subcooling starting at the stagnation point ($\theta = 0$ and $L = 0$ for upward flow and $\theta = 180$ and $L = 0.21$ for downward flow), temperature decreases with increasing arc-length due to increase in velocity and heat transfer coefficient. By developing the laminar boundary layer on the CT surface, the heat transfer coefficient decreases and temperature increases. Eventually, separation occurs and fluid temperature declines due to the increase in the heat transfer coefficient in the wake region. As can be observed from the $k - \omega$ results, the variations in local fluid temperature become smaller as subcooling reduces. Qualitatively, this indicates a greater tendency for vapor film to extend around the CT surface as subcooling decreases. The obtained result shows agreement with the experiments performed under COG (CANDU Owner Groups) funding in which the film boiling patches on the CT surface were obtained mostly at the bottom of the cylinder or on the top of it.

5.2.3 Comparison Between the Two Models

Comparing Figures 4 and 7 which show the temperature distribution around the central CT obtained by $k - \epsilon$ and $k - \omega$ models respectively indicates some differences for the two models' predictions. In $k - \omega$ model the maximum temperature is at the forward stagnation point while in the $k - \epsilon$ model it is at the separation point on the cylinder. At low subcoolings the $k - \omega$ model predicts higher probability of film boiling occurrence at the stagnation point in the front of the cylinder because not only the very low velocity results to accumulation of vapor bubbles but also the higher fluid temperature can lead to more bubble generation at this region. At high subcoolings the large temperature gradient will mitigate against significant vapor accumulation. This should also be noted that in $k - \epsilon$ results the local temperature variations around the cylinder are smaller which means that the change in the local temperature is smoother than the $k - \omega$ predictions. In the $k - \omega$ results there is a sharp change in the temperature at the forward

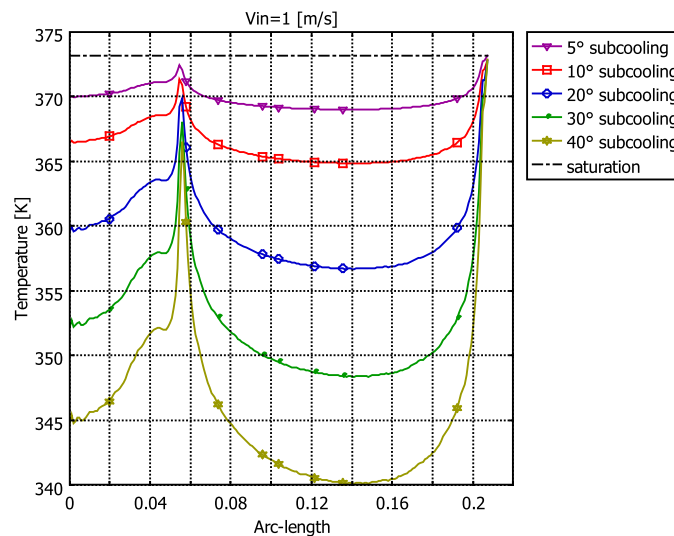


Figure 8. Local temperature around CT for downward flow by $k - \omega$ model

stagnation point and at the separation point.

Comparing Figures 4 and 7 also indicates that in the $k - \omega$ predictions the temperature decreases sharply after the stagnation point from its highest value and it is near constant around the cylinder before the separation point at which the temperature again increases sharply. After the separation point, in the wake region again the temperature decreases due to the flow recirculation in the wake region. Although the same behavior was observed by the $k - \epsilon$ model but the temperature decreases smoothly from the stagnation point and again increases smoothly to reach to the separation point. In fact the high temperature regions predicted by $k - \epsilon$ model are not as localized as the one predicted by $k - \omega$ model. Another important difference between the $k - \epsilon$ and $k - \omega$ models which can be seen from Figures 4 and 7 for upward flow is the significant differences in temperature of the stagnation point in different subcoolings. The same behaviour is observed for downward flow in Figures 5 and 8. This can be explained by the differences in velocity distribution in the two models. Figure 9 (a) and (b) show the velocity streamlines for upward flow obtained by $k - \epsilon$ and $k - \omega$ model, respectively. For the $k - \epsilon$ model, the flow stream in region 2 is extended to the region 1 and it passes through the stagnation point on the bottom of the CT and therefore the fluid subcooling in region 2 affects the temperature of the stagnation point. Therefore the temperature at this point is reduced by increasing in subcooling (see Figures 4). Interestingly, for the $k - \omega$ model, the recirculation zone of the lower channel is extended to region 1 at the bottom of the central CT and the flow stream in region 2 does not affect significantly on that. Therefore the subcooled fluid from region 1 can not reach to the stagnation point and its subcooling does not affect the temperature at this region.

For both turbulent models, by decreasing the inlet velocity, the overall temperature becomes higher especially in downward flow where the effect of buoyancy forces become significant. At very low velocity (0.2m/s), there is a relatively high temperature increase in the wake region for both upward and downward flows.

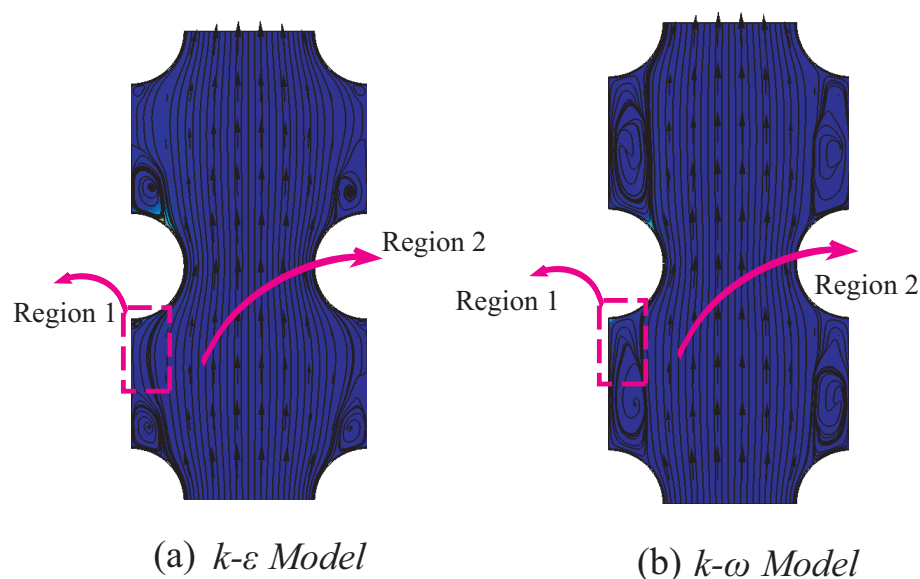


Figure 9. Velocity streamlines for upward flow, (a) $k - \epsilon$ and (b) $k - \omega$ model

6. CONCLUSION

The focus of this research was to establish a Computational Fluid Dynamics (CFD) model for predicting the moderator flow field and temperature distribution around one single channel to investigate the potential of dryout occurrence on the CT surface following a PT/CT contact. Buoyancy forces due to density variations has been taken into account and the fluid is considered to be single phase. Two different turbulent models $k - \epsilon$ and $k - \omega$ have been used separately to predict the fluid turbulence and the obtained results were compared together. The model clearly indicates the wake region behind the cylinder. It also shows the stagnation region in front of the cylinder at which the velocity is zero and it can be concluded that the stagnated flow can result to accumulation of the bubbles and consequent stable vapor film generation at this region. Some major differences were observed in the predictions of the two turbulence models. $k - \omega$ model predicts the highest temperature at the stagnation point in front of the cylinder while $k - \epsilon$ model predicts the highest temperature at the separation point on the cylinder. The predicted local temperature variations with subcooling illustrates a greater tendency for vapor film to extend around the CT surface at low subcooling for both $k - \omega$ and $k - \epsilon$ models. This shows the importance of moderator subcooling in preventing the vapor film to extend on the CT surface. The high temperature regions predicted by $k - \epsilon$ model are not as localized as the one predicted by $k - \omega$ model.

ACKNOWLEDGMENTS

The financial support of the Natural Science and Engineering Research Council (NSERC) and the University Network of Excellence in Nuclear Engineering (UNENE) is gratefully acknowledged.

REFERENCES

1. G. Austman, J. Szymanski, W.I. Midvidy, "MODCIR: A Three-Dimensional Transient Code Used in Thermal-Hydraulic Analysis of CANDU Power Reactor" *Proceedings of the 10th IMACS World Congress on Systems Simulation and Scientific Computatio, Montreal, Quebec*, (1982).
2. G. Austman, J. Szymanski, M. Garceau and W.I. Midvidy, "Measuring Moderator Temperature in a CANDU Reactor", *6th Annual Conference of CNS, Ottawa, Canada*, (1985).
3. C.K. Choo, G. Austman, Y.T. Chan, W.I. Midvidy, "Numerical Simulation of Moderator Circulation in the Calandria Vessel" *Proceedings of the 7th Simulation Symposium on Reactor Dynamics and Plant Control, Montreal, Quebec*, (1980).
4. COMSOL Chemical Engineering Module User's Guide, <http://www.comsol.com>, (2008).
5. H.Z. Fan, Z. Bilanivic, "Use of CATHENA to Model Calandria-Tube/Moderator Heat Transfer After Pressure Tube/Calandria tube Ballooning Contact" *CNS 6th International Conference on Simulation Methods in Nuclear Engineering, Montreal, Quebec, Canada*, (2004).
6. G.E. Gillespie, "An Experimental Investigation of Heat Transfer From a Reactor Fuel Channel to Surrounding Water", *2nd Annual Conference of the Canadian Nuclear Society 1981*, p 157-163, (1981).
7. R.G. Huget, J.K. Szymanski and W.I. Midvidy, "Status of Physical and Numerical Modelling of CANDU moderator circulation", *Proceedings of 10th Annual Conference of Canadian Nuclear Society, Ottawa, Canada*, (1989).
8. R.G. Huget, J.K. Szymanski and W.I. Midvidy, "Experimental and Numerical Modelling of Combined Forced and Free Convection in a Complex Geometry with Internal Heat Generation", *Proceedings of 9th International Heat Transfer Conference, Jeusalem, Israel*, (1990).
9. F. Incropera and D.DeWitt, "Introduction to Heat Transfer", 2nd ed., (1990).
10. W.M. Kays, "Turbulent Prandtl Number. Where Are We?" *Journal of Heat Transfer*, v116, p284-295, (1994).
11. H.F. Khartabil, W.W. Inch, J.K. Szymanski, D. Novog, V. Tavasoli and J. Mackinnon, "Three Dimentional Moderator Circulation Experimental Program for Validation of CFD code MODTURC-CLAS", *21st CNS Nuclear Simulation Symposium, Ottawa, Canada*, (2000).
12. M. Kim, S. Yu and H. Kim, "Analysis on Fluid Flow and Heat Transfer inside Calandria vessel of CANDU-6 using CFD", *Nuclear Engineering and Design*, v236, n11, p1155-64, (2005).
13. B.E. Launder and D.B. Spalding, "Mathematical model of turbulence" *Academic Press.*, London, (1972).

14. J.C. Luxat, "Thermalhydraulic Aspects of Progression to Severe Accidents in CANDU Reactors", *12th International Topical Meeting on Nuclear Reactor Thermalhydraulics (NURETH-12), Pennsylvania, U.S.A., (2007).*
15. H. Schlichting, K. Gersten, "Boundary Layer Theory" *Springer, (2000).*
16. J.K. Szymanski, K.C. Garceau and W.I. Midvidy, "Numerical Modeling of Three-Dimensional Turbulent Moderator Flow in Calandria", *Canadian Nuclear Society/American Nuclear Society International Conference on Numerical Methods in Nuclear Engineering, v2, p970-84, (1983).*
17. T. Von Karman, "Mechanische Ahnlichkeit und Turbulenz" *Third Int. Congr. Applied Mechanics, Stockholms, p85-105, (1930).*
18. D.C. Wilcox, "Turbulence Modeling for CFD", *DCW Industries Inc., (1998).*
19. O.C. Zienkiewicz, R.L. Taylor, P. Nithiarasu, "The Finite Element Method for Fluid Dynamics" *Elsevier Butterworth-Heinemann, Oxford, (2005).*
20. A. Zukauskas, J. Ziugzda, "Heat Transfer of a Cylinder in Crossflow" *Hemisphere Pub, Washington; New York, (1985).*